Microbiology, Vol. 71, No. 3, 2002, pp. 306–313. Translated from Mikrobiologiya, Vol. 71, No. 3, 2002, pp. 359–367.

EXPERIMENTAL ARTICLES

Defective Lysogeny in *Erwinia carotovora*

F. I. Tovkach

Zabolotnyi Institute of Microbiology and Virology, National Academy of Sciences of Ukraine, ul. Zabolotnogo 154, Kiev, 03143 Ukraine

Received August 30, 2001

Abstract—The electron microscopic study of several *Erwinia carotovora* strains showed that the SOS-induced cells of this pectolytic phytopathogenic bacterium produce particular phage parts (tails, heads, and baseplates) but do not assemble them into fully functional phage particles. *E. carotovora* cells produced several times greater amounts of phage tails in response to induction by mitomycin C than in response to induction by nalidixic acid. The tails were 128–192 nm in length and 13–21 nm in diameter. Phage heads were characterized by four discrete ranges of diameters: 18, 55–59, 66–75, and 92–98 nm. The diameters of phage baseplates varied from 39 to 53 nm, depending on the particular strain. It was shown that cells of the same species may contain several different types of phage tails and heads. The structural organization of phage tails and baseplates in the nalidixic acid–induced lysate of *E. carotovora* J2 was studied in more detail. The data obtained suggest that pectolytic phytopathogenic erwinia are characterized by defective polylysogeny.

Key words: Erwinia carotovora, defective lysogeny, phage particles, electron microscopy.

There are two types of bacterial lysogeny, true and defective [1, 2]. True lysogeny implies that the prophages of temperate bacteriophages may convert to either a lysogenic or vegetative state, while defective lysogeny implies that the prophages cannot convert to fully functional phages because of some genetic defects. The common products of defective phage assembly are tail parts, which attract the attention of researchers due to their killer activity with respect to susceptible bacterial species [3–5]. At the same time, other parts of phages (heads and baseplates) have not yet been adequately investigated.

Many macromolecular carotovoricins (MCTVs) of the phytopathogenic bacterium *E. carotovora* are bacteriophage tail–like particles [3, 6–8], which allowed the suggestion to be made that this bacterium is characterized by defective lysogeny.

The present work is an attempt to reveal defective lysogeny in some phytopathogenic strains of *E. carotovora*.

MATERIALS AND METHODS

Experiments were carried out with eight *Erwinia carotovora* subsp. *carotovora* strains (ECA 4A, ECA 35A, ECA 48, ECA 62A, ECA 59A, ECA M2-4, ECA Ec153 (ATCC 15359), and ECA J2 (NCPPB 1744)), two *Erwinia aroideae* strains (EAR g48 and EAR 3A), and one *Erwinia* sp. ZM-1 strain (ESP ZM-1). The first ten strains were obtained from Yu.K. Fomichev, Department of Microbiology, Belarussian University, Minsk. The last strain was isolated in our laboratory from a potato tuber affected by soft rot [9].

To obtain bacterial lysates with phage particles, erwinia cells were treated with 1 μg/ml mitomycin C or 20 μg/ml nalidixic acid [8]. The lysate (200 ml) of each of the strains was centrifuged twice in a Spinco L8-70 centrifuge with an SW28 rotor at 24 000 rpm for 80 min. The pellet of phage particles was suspended in 1 ml of ST buffer (50 mM Tris–HCl, pH 7.5, with 10 mM NaCl). The phage particles of strain ECA 35A were additionally purified by gel filtration on a Sepharose 2B column (8×200 mm).

The electron microscopic studies of phage particles contrasted with 2% uranyl acetate were carried out using an EMB 100BP electron microscope. Particle sizes were evaluated from the electron images of T4D bacteriophage tails, which have a standard length of 113 nm. All electron images were obtained at a magnification of 240000× to 280000×.

RESULTS

Detection of phage parts in the antibiotic-induced *E. carotovora* lysates. Almost all spontaneous and induced *E. carotovora* lysates were found to contain particular parts of phage particles (tails, heads, and baseplates). Figure 1 presents the electron microscopic images of particles found in the mitomycin C–induced *E. carotovora* lysates purified by repeated ultracentrifugation. The particles were identified as normal tails (NTs), tails with contracted sheaths (CSs), tail tubes (TTs), phage heads (PHs), and baseplates (BPs).

The relative numbers of various phage parts in the induced lysates of four *E. carotovora* strains are presented in Table 1. It can be seen that the SOS induction

0026-2617/02/7103-0306$27.00 © 2002 MAIK "Nauka / Interperiodica"

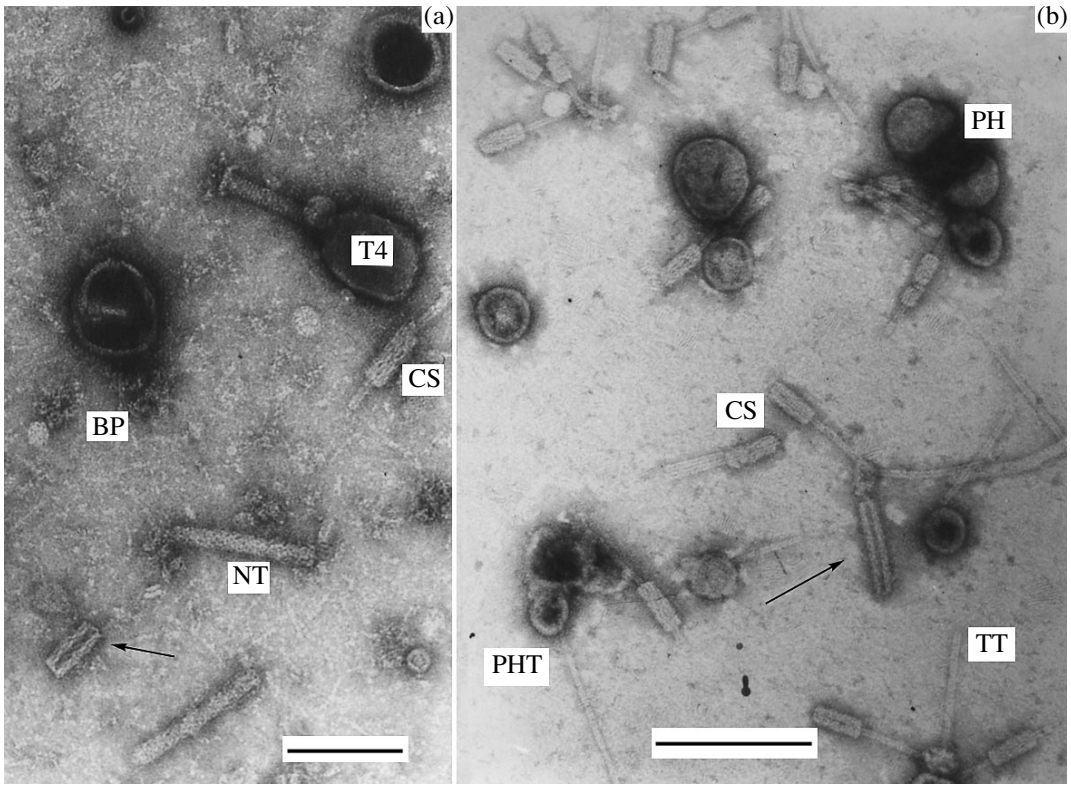

Fig. 1. Electron images of the phage parts found in the mitomycin C–induced lysates of *E. carotovora* strains (a) ECA Ec153 and (b) ECA 35A. NT, normal tail; CS, tail with a contracted sheath; PH, phage head; PHT, phage head associated with a long rigid tail tube; TT, free tail tube; BP, baseplate; T4, bacteriophage T4D particle. The arrows point to hollow sheaths. Scale bars represent (a) 100 nm and (b) 200 nm.

of *E. carotovora* cells gave rise to all major phage elements. The content of phage tails in the mitomycin-induced lysates was greater than in the nalidixic acid–induced lysates. Conversely, the content of baseplates was greater in the nalidixic acid–induced lysates. The relative content of phage heads did not depend on the inducer and varied from 1% in the lysate of strain ECA Ec153 to 17% in the lysate of strain ECA 35A. The percentage of phage tails with normal (noncontracted, relaxed) sheaths varied from 3 to 11%. Almost all *E. carotovora* lysates contained hollow sheaths of different lengths (Fig. 1).

Phage tail parts in *E. carotovora* lysates. Unlike normal phage tails, CS particles found in *E. carotovora*

Table 1. Relative content of various phage parts in the *E. carotovora* lysates induced with mitomycin C (MC) and nalidixic acid (NA)

Phage part	Strain				
	ECA J2		ECA 62A	ECA 35A	ECA Ec153
	NA	MC	NA	MC	MC
Total tail parts	10	76	33	59	28
normal tails	3	7	11	0	4
tails with contracted sheaths	7	49	21	38	24
tail tubes	0	20	1	21	0
hollow sheaths	3	2	0	4	36
Baseplates	85	20	63	20	35
Phage heads	2	2	4	17	1
Total number of particles in one microscope field	179	43	237	48	42

Table 2. Clustering of the phage tails with contracted sheaths (CS particles) of three *E. carotovora* strains with respect to the modal volume V_m

Sheath parameters	Strain		
	ECA 35A	ECA Ec153	EAR 3A
N	46	44	63
Mean values and deviations, nm*			
L	62.0	55.5	69.8
σl_n	3.6	3.0	3.1
W	23.5	20.0	26.5
σw_n	1.6	1.7	1.5
Type I			
V_{m1}, $\times 10^3$ nm^3	22.8	14.1	36.6
f_1, %	26.0	36.0	38.0
L_1, nm	61.0	54.4	70.0
W_1, nm	21.8	18.3	25.9
Type II			
V_{m2}, $\times 10^3$ nm	26.8	20.0	41.8
f_2, %	20.0	32.0	19.0
L_2, nm	62.9	57.3	68.5
W_2, nm	23.4	21.0	28.0
Type III			
V_{m3}, $\times 10^3$ nm	30.5	–	–
f_3, %	17.0	–	–
L_3, nm	60.1	–	–
W_3, nm	25.4	–	–

* Presented are the mean length (L) and width (W) of sheaths and their standard deviations σl_n and σW_n for the general data array N. The sheaths were grouped according to three discrete modal volumes V_{m1}, V_{m2}, and V_{m3}. F is frequency at the maximum of the Gauss distribution curve. "–" stands for "not detected."

lysates tended to destruction in two particular stages, the stage of sheath swelling followed by the stage of sheath rupture along the long axis. For this reason, the CS particles that had conspicuous lesions were not taken into account during analysis. The length (L) and the width (W) of CS particles were characterized by considerable standard deviations σ_n, which varied from 4 to 6% for L and from 5 to 9% for W. These data, together with the observation that CS particles may have different arrangements of structural subunits of their sheaths, allowed the suggestion to be made that the phage tails of the same *E. carotovora* strain may be of several types. The statistical analysis of CS particles in terms of the volume of a cylinder with diameter W and height L showed that these particles in the lysates of particular *E. carotovora* strains could be characterized by up to three modal volumes V_m. This made it possible to identify three types of CS particles in the mitomycin C–induced lysates of three *E. carotovora* strains (Table 2).

A similar statistical analysis with respect to the length and width of normal tails with relaxed sheaths, the length of tail tubes, and the diameters of phage heads and baseplates showed that the lysates of all *E. carotovora* strains studied contained at least two types of NTs (Table 3), whose length varied from 128 to 192 nm and whose width varied from 15 to 21 nm. The length of the tail tubes, either naked or covered with contracted sheaths (Fig. 1b), was equal to that of NTs (Table 3). The contraction of tail sheaths shortened their length to 43–70 nm and increased their diameter to 16–28 nm. The lysates of some strains did not contain NTs. Experiments in vitro showed that normal tails spontaneously convert into tails with contracted sheaths, i.e., into CS particles. The presence of TTs and the variable length of tail tubes covered with contracted sheaths can be explained by the general instability of phage tails, which may easily break during the preparation of phage suspensions.

Electron microscopic analysis and the study of the killer activity of NTs with respect to susceptible bacterial cells showed that these phage parts actually represent tail-like carotovoricins (TLCA), which are able to kill susceptible *E. carotovora* cells after adsorption on the cell surface. The antibiotic-induced lysates of strain ECA J2 contained at least three types of TLCA.

One of the TLCA types, TLCA 44-1, in a relaxed state had a length of 128 nm and a width of 16 nm (Fig. 2a) and exhibited several variants of contracted sheath (Figs. 2c–2e, 2h, 2i). The apical region of the contracted sheath of TLCA 44-1, located at a distance of 16–47 nm from its proximal end, represented a special structure, which was named abnormal sheath (ANS). The structure of ANS differed from that of the rest of the sheath. The average dimension of ANSs was 19.5×18.2 nm. The ANS of TLCA 44-1 was the first to contract and then stimulated the contraction (Figs. 2e, 2i) or caused the destruction (Figs. 2h) of the distal part of the sheath. These data suggest that the ANS of TLCA 44-1 may contain a specific structural protein, differing from that of the distal part of the sheath.

The second type of TLCA found in the lysates of strain ECA J2, TLCA 44-2, had approximately the same length as TLCA 44-1 but a narrower width (W = 13.4 nm) (Fig. 2b). The structural subunits of the contracted sheath of TLCA 44-2 were characterized by an arrangement (Fig. 2g, 2) different from that of the contracted sheath of TLCA 44-1. The average dimension of TLCA 44-2 was 49.4×17.0 nm.

The third type of TLCA, TLCA 44-3, was distinguished by the presence of a naked tube at the sheath apex (Fig. 2f). TLCA 44-3 had an average length of 153.6 nm and an average width of 15.0 nm and often exhibited a segmentation of the contracted sheath (Fig. 2g, 1). The mean length of the TLCA 44-3 tube

Table 3. Mean linear sizes (in nm) of the phage tails found in the induced lysates of *E. carotovora* strains

Strain	Tail type	Normal tail		Tail with contracted sheath		
				sheath		tube
		L	*W*	*L*	*W*	*L*
ECA 35A	TLCA 12-1	–	–	61.0	21.8	150.0
	TLCA 12-2	–	–	62.9	23.4	159.0
	TLCA 12-3	–	–	60.1	25.4	–
ECA J2	TLCA 44-1	128.0	15.1	–	20.0	127.2
	TLCA 44-2	128.6	13.4	49.4	17.0	122.0
	TLCA 44-3	153.6	15.0	68.4	20.2	134.0
ECA 62A	TLCA 5-1	135.5	15.1	–	–	134.7
	TLCA 5-2	147.5	17.2	58.3	19.0	146.4
	TLCA 5-3	–	–	–	–	160.5
ECA Ec153	TLCA 29-1	135.8	15.9	54.4	18.3	134.0
	TLCA 29-2	146.2	17.3	57.3	21.0	147.5
ECA 48A	TLCA 25-1	161.0	16.4	68.5	21.1	160.0
	TLCA 25-2	–	–	66.8	26.8	–
EAR 3A	TLCA 11-1	187.0	18.8	70.0	26.0	–
	TLCA 11-2	192.0	21.6	68.5	28.0	–
ESP ZM-1	TLCA 40-1	184.0	–	–	–	–
	TLCA 40-2	–	–	52.8	16.4	–
EAR g48	TLCA 2-1	–	–	58.3	21.5	–
	TLCA 2-2	–	–	61.6	25.4	–
ECA 59A	TLCA 55-1	–	–	55.3	21.8	–
	TLCA 55-2	–	–	61.4	17.2	–
ECA 4A	TLCA 36-1	–	–	66.4	24.7	–
	TLCA 36-2	–	–	68.0	27.3	–
ECA M2-4*	TLCA 50-1	–	–	42.9	14.3	–

Note: "–" stands for "no data available."

* Mean sizes were calculated for 10 particles.

was 134 nm, i.e., it was shorter than the normal phage tails of *E. carotovora.*

It should be noted that this consideration of the structure of TLCAs is quite tentative. The spontaneous destruction of the tail tubes (Figs. 2d, 2e), the different states of contracted sheath subunits at the opposite ends of the sheaths (Figs. 2c–2e, 2h, 2i), and the elaborate arrangement of the contracted sheaths of TLCA 44-1 and TLCA 44-3 (Figs. 2g, 2i) did not allow the structure of NT and CS phage particles to be analyzed in depth.

Phage heads and baseplates in the antibiotic-induced lysates of *E. carotovora*. As mentioned above, the lysates of strain ECA 35A contained the greatest amounts of phage head–like particles (Table 1 and Fig. 1b). The statistical analysis of these particles showed that they fall into three categories (Table 4). Some phage heads were polar (Fig. 3a). Small heads with a modal diameter of 55.4 nm were typically associated with one or two segmented rigid tubes 94 to 226 nm in length (Figs. 1b, 3a, PHT). In this strain, most of the phage heads were likely filled with a nucleic acid of unknown origin.

The lysates of strain ECA Ec153 contained two types of phage heads (Table 4), empty heads 66.2 nm in diameter and small heads with a mean diameter of 18.7 nm, which were associated with the normal tails

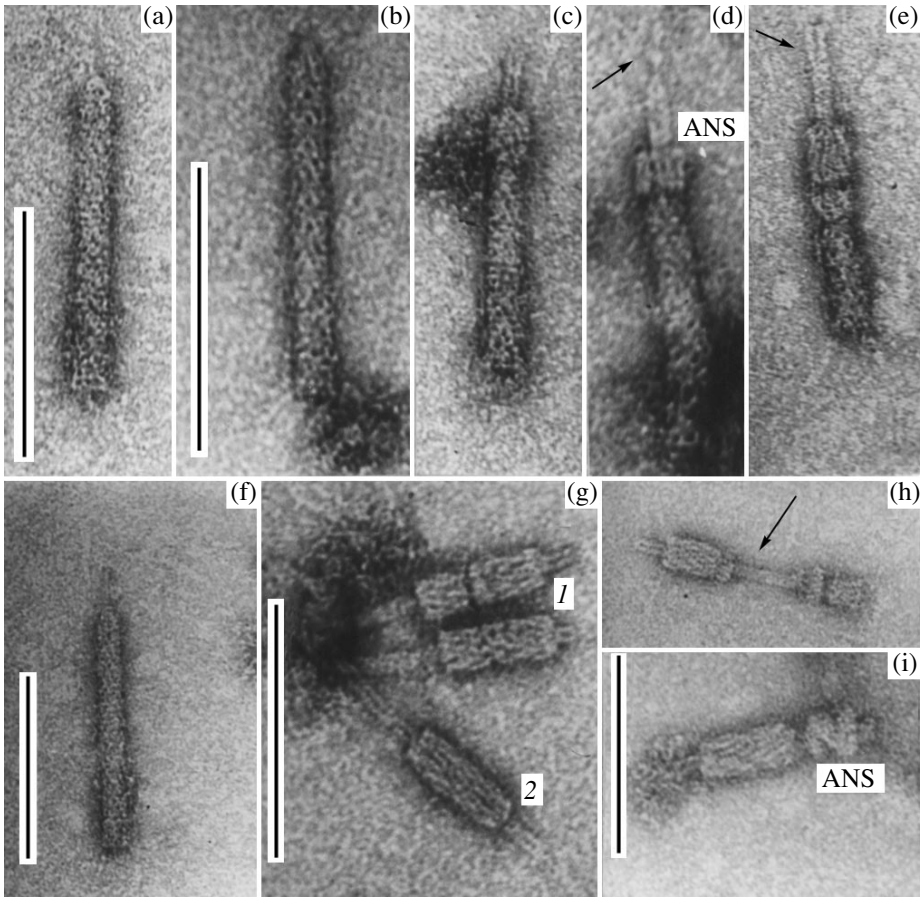

Fig. 2. Electron images of the phage tail–like carotovoricins (TLCA) of three different types found in the induced lysates of *E. carotovora* strain J2: (a) TLCA 44-1; (b) TLCA 44-2; (f) TLCA 44-3; (c–e, h, i) different structural forms of the contracted sheath of TLCA 44-1; (g) the contracted sheaths of (*1*) TLCA 44-3 and (*2*) TLCA 44-2. ANS is the proximal part of the TLCA 44-1 sheath (for details, see text). The arrows point to (d) the disintegrating proximal part of the tail tube and (h) the distal part of the sheath. Scale bars represent 100 nm. Images (a, c, e), (b, d), and (f–h) were obtained at three different magnifications.

TLCA 29-1 and TLCA 29-2, respectively (Figs. 3c, 3d). In the mitomycin C–induced lysate of this strain, similar small heads bound to anomalously long (417 nm) tails through a system of thin fibers could be sometimes observed (Fig. 3b). The ECA 62A lysates contained primarily empty ellipsoidal heads with a mean diameter of 92 nm, some of which were associated with the normal TLCA 5-1 tails (Fig. 3e). None of the *Erwinia* strains investigated contained fully assembled bacteriophages or phage heads bound to tails covered with contracted sheaths.

Table 4. Diameters of the phage heads and baseplates found in the lysates of some *E. carotovora* strains

Strain	Head diameter, nm				Baseplate diameter, nm
	Type I	Type 2	Type 3	Type 4	
ECA 35A	–	55.4	75.0	98.2	–
ECA J2	–	59.0	67.0	–	39.7
ESA Ec153	18.7	–	66.2	–	45.6
ECA 62A	–	–	–	92.0	44.5
ECA 48A	–	–	–	–	50.0
ECA 4A	–	–	–	–	53.0

Note: "–" stands for "no data available."

All erwinia lysates were found to contain a great number of baseplate-like particles (Table 1 and Figs. 4a, 4b). The baseplates could be easily separated from other phage parts by gel filtration on Sepharose 2B. Many baseplates possessed hexagonal symmetry (Figs. 1a, 4a). The diameter of baseplates ranged from 39.7 to 53 nm (Table 4) and was proportional to the width of normal tails. Some normal tails lacked baseplates but were furnished with short fibers on their distal ends (Figs. 2a, 2b, 2f).

The elaborate phage heads of strain ECA J2, designated as BPJ, were studied in more detail. They were either free or bound to the distal part of the TLCA 44-3 particles (Fig. 4c). Free BPJ could occur in three conformational states of a *bicycle wheel* (Fig. 4d, 1), a ran-

domly coiled *globule* (Fig. 4d, 2), and a symmetric round *tangle* with a distinct central part (Fig. 4d, 3). When BPJ occurred in the two last states, it tended to form a structure with six paired rigid fibers 56–58 nm in length (Fig. 4e, F). The mean diameter of BPJ was found to be 39.8 nm with a standard deviation of 4 nm, which agrees with a modal diameter of 39.7 nm (σd_n = 1 nm) well. The origin and the relationship between the four different types of baseplates in *E. carotovora* strain J2 need further investigation.

DISCUSSION

The data presented in this study show that bacteriocinogeny and defective lysogeny in pectolytic phytopathogenic *E. carotovora* strains are closely related. The killer factors of this bacterium represent the intermediate products of the incomplete assembly of defective temperate bacteriophages in SOS-induced lysogenic cells. The SOS induction of erwinia cells with mitomycin C or nalidixic acid resulted in the formation of phage tails, heads, and baseplates (Figs. 1, 3, 4) in proportions dependent on the antibiotic used for induction (Table 1). In response to induction with nalidixic acid, *E. carotovora* cells produced from 63 to 85% of phage baseplate–like particles. The mechanism of this phenomenon remains unknown and needs further study. In response to induction with mitomycin C, *E. carotovora* cells primarily produced phage tail–like particles, whose relative content varied from 28 to 76%, depending on the particular strain.

The *E. carotovora* strains under study produced three different types of phage tails (Tables 2 and 3), differing in linear sizes and structural organization (Fig. 2), as well as four different types of phage heads (Table 4 and Fig. 3). One of the strains (ECA 35A) was found to produce three different types of phage heads. These data strongly suggest that phytopathogenic pectolytic erwinia are subject to defective polylysogeny and confirm the multiplicity of macromolecular carotovoricins, which was revealed earlier during the study of carotovoricin-resistant bacterial mutants [11].

Some suppositions can be made about the defects in the prophage genomes of *E. carotovora* that are responsible for the incomplete assembly of phage particles in this bacterium. First, this can be related to the altered synthesis of a connective material, due to which the DNA-containing phage heads and tails are either unbound (as in strain ECA 35A) or loosely bound (as in strain ECA Ec153) (Fig. 3). Second, some defects may occur in the package of DNA in phage heads, as is evidenced by the formation of defective heads in the strain ECA Ec153 and of empty heads in the strain ECA 62A. Third, the phage parts observed in the induced lysates of *E. carotovora* may be the products of particular genetic elements of defective prophages located in different regions of the bacterial chromosomes and unrelated structurally and functionally. This suggestion follows from the excessive synthesis of phage baseplates

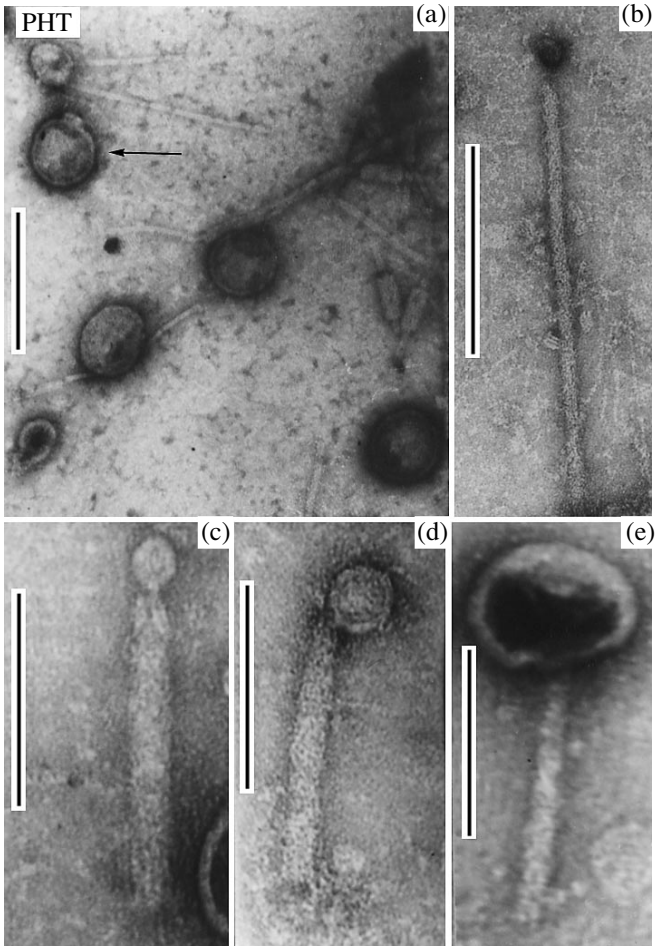

Fig. 3. Electron images of the phage heads found in the lysates of (a) ECA 35A, (b–d) ECA Ec153, and (e) ECA 62A. PHP, phage head associated with two rigid tail tubes. The arrow points to a polar head. Scale bars represent (a, b) 200 nm and (c–e) 100 nm.

in most of the *E. carotovora* strains studied (Table 1 and Fig. 4).

Some phage particles described in this paper have not yet been described in the literature. These are the small heads associated with one or two long rigid tail tubes found in strain ECA 35A (Figs. 1 and 3), the binary sheaths of TLCA 44-1 and TLCA 44-3 particles (Fig. 2), and the elaborate baseplates PBJ found in strain ECA J2 (Fig. 4).

The data presented in Table 4 suggest that the heads of defective temperate phages are close in shape to the heads of isometric phages. This, together with the fact that all of the tails found in the *E. carotovora* lysates are contractile, allows another suggestion to be made. Namely, the defective temperate bacteriophages of *E. carotovora* belong to morphotype A1. It should be noted in this regard, that the new temperate bacteriophage ZF40 of *E. carotovora* [12] also belongs to this morphotype, although it differs from the defective

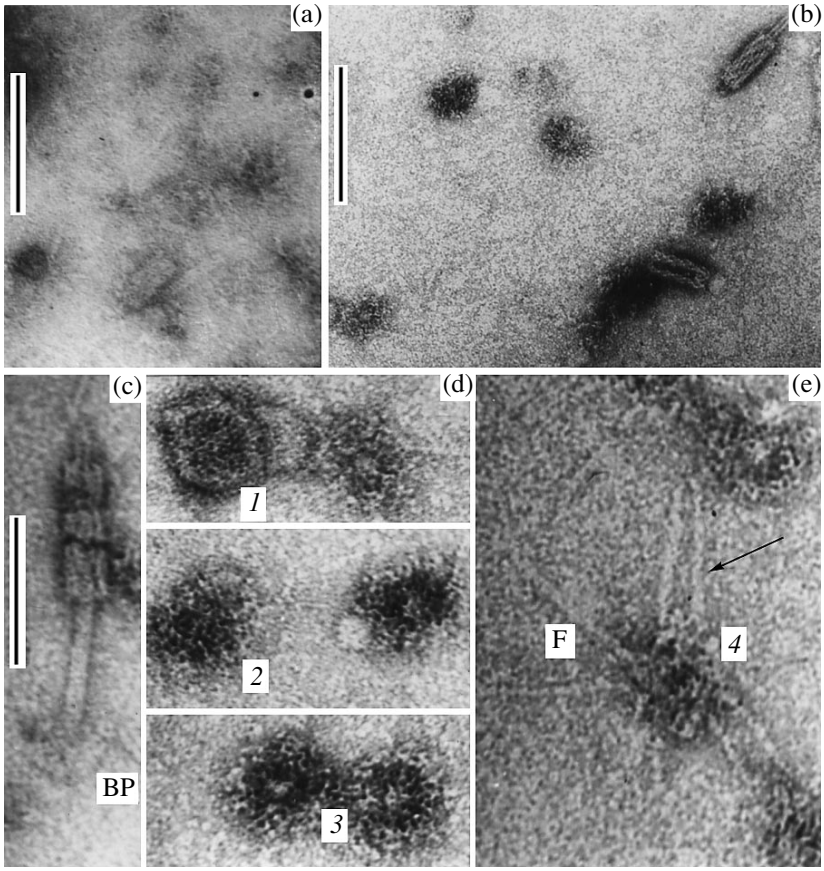

Fig. 4. Baseplate-like particles found in the lysates of (a) ECA 4A and (b–e) ECA J2 induced with (a) mitomycin C and (b) nalidixic acid. BP, baseplate associated with the distal end of TLCA 44-3; *1–4*, different conformations of BPJ (see text for details); and F, fibers associated with a baseplate. The arrow points to the paired fibers of BPJ. Scale bars represent (a, b) 100 nm and (c–e) 50 nm.

phage particles described in the present paper in the size and structure of the contractile sheath.

The lengths of the defective phage tails found in the lysates of the *E. carotovora* strains under study (128 to 192 nm) are close to the lengths of the phage tails found in other *E. carotovora* strains [3, 14], as well as to the lengths of the R-type pyocins [14] and the macromolecular bacteriocins of other bacteria [4].

The data obtained suggest that pectolytic phytopathogenic erwinia persist in nature as defective polylysogenic systems. Defective polylysogeny in *E. carotovora* is closely related to the phage tail–like macromolecular carotovoricins.

REFERENCES

1. Campbell, A., Comparative Molecular Biology of Lambdoid Phages, *Annu. Rev. Microbiol.*, 1994, vol. 48, no. 1, pp. 193–222.
2. Prozorov, A.A., Defective Balillar Phages: Cell Parasites or Chromosome Components?, *Genetika*, 1996, vol. 32, no. 4, pp. 469–481.
3. Itoh, Y., Izaki, K., and Takahashi, H., Purification and Characterization of a Bacteriocin from *Erwinia carotovora*, *J. Gen. Appl. Microbiol.*, 1977, vol. 24, no. 1, pp. 27–39.
4. Boemare, N.E., Boyer-Giglio, M.-H., Thaler, J.-O., Akhuerst, R.J., and Brehelin, M., Lysogeny and Bacteriocinogeny in *Xenorhabdus nematophilus* and Other *Xenorhabdus* spp., *Appl. Environ. Microbiol.*, 1992, vol. 58, no. 9, pp. 3032–3037.
5. Lee, F.K.N., Dudas, K.S., Hanson, J.A., Nelson, P.T., and Apicella, M.A., The R-Type Pyocin of *Pseudomonas aeruginosa* C Is a Bacteriophage Tail–Like Particle That Contains Single-stranded DNA, *Infect. Immun.*, 1999, vol. 67, no. 2, pp. 717–725.
6. Tovkach, F.I., Grigoryan, Yu.A., Ruban, V.I., and Kishko, Ya.G., Polylysogeny in *Erwinia carotovora* 268 R, *Mikrobiol. Zh.*, 1984, vol. 46, no. 3, pp. 7–78.
7. Crowly, C.F. and DeBoer, S.H., Sensitivity of Some *Erwinia carotovora* Serogroups to Macromolecular Bacteriocins, *Can. J. Microbiol.*, 1980, vol. 26, no. 9, pp. 1023–1028.
8. Tovkach, F.I., Biological Properties and Classification of *Erwinia carotovora* Bacteriocins, *Mikrobiologiya*, 1998, vol. 67, no. 6, pp. 767–774.
9. Gorb, T.E. and Tovkach, F.I., Typing *Erwinia carotovora* Phytopathogenic Strains on the Basis of Pectinolytic

Activity and Sensitivity to Bacteriocins (Carotovoricins), *Mikrobiologiya*, 1997, vol. 66, no. 6, pp. 823–828.

10. Ackermann, H.-W. and Krisch, H.M., A Catalogue of T4-Type Bacteriophages, *Arch. Virol.*, 1997, vol. 142, no. 12, pp. 2329–2345.
11. Tovkach, F.I., Relationship between the Lytic Activity of Macromolecular Carotovoricins and Bacteriocin Sensitivity of Producer Strains of *Erwinia carotovora*, *Mikrobiologiya*, 1998, vol. 67, no. 6, pp. 775–781.
12. Tovkach, F.I., Structural Organization and Restriction DNA Analysis of the Temperate Bacteriophage ZF40 of *Erwinia carotovora*, *Mikrobiologiya*, 2001, vol. 71, no. 1.
13. Nguyen, A.H., Tomita, T., Hirota, M., Sato, T., and Kamio, Y., A Simple Purification Method and Morphological and Component Analyses for Carotovoricin Er, a Phage Tail–Like Bacteriocin from the Plant Pathogen *Erwinia carotovora* Er, *Biosci. Biotechnol. Biochem.*, 1999, vol. 63, no. 10, pp. 1360–1369.
14. Kageyama, M., Shinomiya, T., Aihara, Y., and Kobayashi, M., Characterization of a Bacteriophage Related to R-Type Pyocins, *J. Virol.*, 1979, vol. 32, no. 3, pp. 951–957.